EROSION PROCESSES IN COMPOSITE RIVERBANKS: EXPERIMENTS AND MODELLING

Subashisa Dutta[1], Tapas Karmakar[2]

[1]*Professor, Indian Institute of Technology Guwahati*
subashisa@iitg.ernet.in
[2]*Assistant Professor, Thapar University, Patiala*
tapas1976@gmail.com

Abstract

Erosion processes in a composite bank is a very complex phenomenon due to many factors involved such as: seepage, variability of the bank stratifications, river stage variations, fluvial processes, soil stabilities. This study was focused to understand the primary processes responsible for bank erosion, and methodology to predict the bank erosion. Finally, a stochastic bank erosion model is proposed to estimate the seasonal bank erosion in a composite river bank. In the first stage, the developed model was simulated with known stage hydrograph, bank soil erodibility, and the bank stratification of a river bend in a reach of the Brahmaputra River in India. The critical shear stresses of the bank soils were determined through submerged-jet tests and the seepage erosion parameters were determined through laboratory lysimeter experiments. The predicted seasonal bank erosion rates for four consecutive years were compared with the observed rates. The results showed a good agreement between the observed data and modelling results. In the second stage, the uncertainty in the stage hydrograph, soil erodibility and the bank stratifications were considered. The stochastic bank erosion predictions were compared with the observed distribution of the bank erosion in 45 bends of the Brahmaputra River over 700 km long reach. Since the model has predicted satisfactorily therefore, the developed model can be used to obtain morphological dynamics of a sand-bed river bend with composite banks.

Keywords*: Bank Erosion, Composite Banks, Fluvial Hydraulics and Brahmaputra*

----------***----------

1.INTRODUCTION

Fluvial bank erosion is a very common phenomenon in alluvial rivers and almost all the rivers in the world is facing severe threats of bank erosion. In cases, where the banks are composed of alternate layers of fine and course strata, the banks are known as composite banks. The bank erosion, especially composite river banks is very complex as the banks are associated with many controlling variables. Since these controlling variables are associated with uncertainty in their measurements therefore, it is difficult to model bank erosion in a large river (Karmaker and Dutta, 2009). River bank erosion occurs mainly due to three processes: fluvial entrainment, sub-aerial erosion and mass failure due to poor strength of the bank materials (Lawler, 1995). One or the combination of these processes is responsible for the river bank erosion. The bank erosion for a homogeneous bank is mainly dominated by a single process. For example, in cohesive soil, slip circle failure often takes place, whereas in sandy cohesionless soil, planer failure is the reason. However, the nature of the erosion for a cohesive river bank is completely different from cohesionless (sand-bed) river bank. In a cohesive river bank, the erosion takes place as aggregates of soil rather than individual particles, as they are bound tightly by the electromechanical cohesive forces (Lawler et al., 1997). On the other hand the erosion in cohesionless river bank is due to loss of individual particles. The river bank erosion in case of a composite river bank is very complex. Banks of the alluvial river reaches are mostly composed of stratified soil layers, grain sizes of which vary from fine to coarse one. Normally, the alluvial river bed and the lower layers of composite banks are composed of cohesionless materials and the top layer of the bank is composed of fine soil with vegetation cover.

Research studies have been carried out to understand or quantify the bank erosion rate in a river either through field and laboratory experiments or through numerical modeling. However, field investigation of the composite bank erosion has focused in the last two decades only. Theoretical study of the mechanical processes of channels with erodible banks was investigated initially by Ikeda et al. (1981) and Parker et al. (1982). Darby and Thorne (1996), Duan (2005), and Chen and Duan (2006) developed the numerical bank erosion models in which the rotational slip and planar bank failures were considered. The model predictions were verified by Darby et al. (1996) with the bank erosion data collected from South Fork Forked Deer River (SFFDR) in west Tennessee. The average longitudinal slope of the river was 1 in 6250 with average top width ~36 m and depth ~4 m. The river bed was composed with well sorted sand (d_{50} = 1 mm). Recent research study on bank erosion model emphasizes on the fluvial erosion and finite element based seepage analysis due to the variation of pore water pressure (Rinaldi et al., 2004; Darby et al., 2007; Rinaldi et al., 2007). Those predictions were well validated with data from the natural river with composite bank. All the cases, the planar failure and/or cantilever failure were considered for bank stability analysis. Seepage erosion study was carried

out to quantify the erosion by several researchers through the laboratory and in-situ seepage experiments (Fox et al., 2006; Wilson et al., 2007; Fox and Wilson, 2010; Midgley et al., 2012b; Rinaldi and Nardi et al., 2012). Karmaker and Dutta (2013) developed seepage erosion model based on stage variation in the river. In that study, a functional relationship between seepage erosion rate and its controlling variables was developed using lysimeter experiments. The relationship was used to formulate a mathematical seepage model that predicts the daily seepage erosion rate for a composite river bank. The results indicated that the seepage gradient has a dominating effect on the time taken in developing undercuts that lead to the bank collapse. They reported that the time to collapse increased significantly with the number of silt layers in the bank profile. Limited studies so far have been carried out for composite riverbank, e.g., BSTEM (Simon et al., 2000) and CONCEPTS (Langendoen, 2000) were developed by the National Sedimentation Laboratory in Oxford, Mississippi, USA. However, both the models do not have the seepage bank erosion component.

In the present study a detailed bank erosion model has been developed for the composite river bank considering the entrainment and deposition of the sediment particle from the bank surface, basal erosion due to excess shear stress, cantilever mass failure and near bank net sediment transport rate and the seepage erosion (Fox et. al., 2007). The objectives of this study were to (i) couple the analytical bank erosion and bed degradation model described by Chen and Duan (2005) and Karmaker and Dutta (2010b) with seepage erosion model (Karmaker and Dutta, 2013) in a composite river bank, (ii) evaluate its performance at a river bend for known soil parameters and hydrographs with *in-situ* bank erosion measurement , and (iii) evaluate its stochastic prediction ability with observed cumulative distribution of the average annual bank erosion rate from the river bends in the Brahmaputra by considering the soil parameter distribution and stochastic stage hydrograph series (Karmaker and Dutta, 2010a).

2. STUDY AREA

The study reach in the Brahmaputra River is selected for the model performance evaluation and located at Jamuguri, North Lakhimpur, North-East India. The reach (26°50'08" N, 93°46' 08" E) is about 70 km upstream of Tezpur town. The river flows from east to west at this location (Fig. 1). Morphological studies using multi-date satellite imagery show that until year 2008 the river bank was under severe threat of erosion. It was also found from the satellite imagery study that a bank area of 2.4 km^2 was eroded out during the flood season of 2004. The radius of the centerline of the bend was about 2460 m and the channel widths at the upstream and downstream were 630 m and 1126 m, respectively (Karmaker and Dutta, 2009).

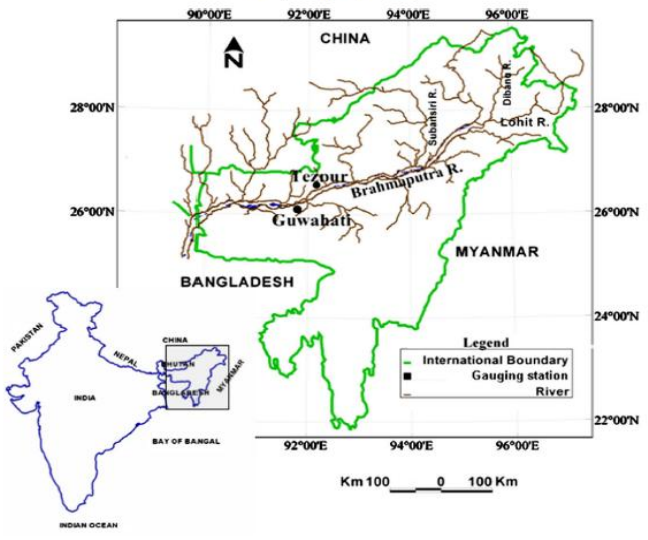

Figure 1. Map showing the Brahmaputra River, Assam (Image is taken from Karmaker and Dutta, 2010)

Hydrographic and river bank surveys with Echo-sounder, acoustic Doppler current profiler (ADCP) were conducted during the moderate and high flow conditions (the water level was nearly 1 m higher than the bank full discharge) for the years 2005, 2006, 2007 and 2008. The measuring devices were mounted on an engine propelled vessel. The accuracy of the GPS instrument was ± 1.5 m. The maximum height of the eroding banks ranged between 8 to 9 m. The longitudinal bed slope varied spatially and temporally and found in between 1 in 7500 to 1 in 10,000. Although the thickness of different layers of the bank formation were found variable, but the average bank composition can be described as (from top to the bottom): (1) a stiff cohesive layer with grass (thickness ~100-150 cm), (2) a layer of densely packed silt (thickness ~25-30 cm), (3) a layer of silty clay (thickness ~40-50 cm), (4) a layer of fine sand (~40-50 cm), (5) a layer of sandy silt (thickness ~300 cm), (6) below that a layer of silty-clay at the bank toe (Karmaker and Dutta, 2011).

3. MODEL FOR BANK EOROSION

3.1 Hydrodynamic Model

The governing equations for water flow in a curved river are the Navier-Stokes equations under depth averaged steady-flow assumptions in two-dimension (Chen and Duan, 2006):

$$\frac{\partial (hu)}{\partial s} + \frac{\partial}{\partial n}\left[(1+nC)hv\right] = 0 \qquad \text{(Eqn.1a)}$$

$$\frac{1}{1+nC}u\frac{\partial u}{\partial s} + v\frac{\partial u}{\partial n} + \frac{C}{1+nC}uv = \frac{-1}{1+nC}g\frac{\partial \xi}{\partial s} - C_f u\frac{\sqrt{(u^2+v^2)}}{h} - \frac{1}{h}\left[\frac{\partial}{\partial n}\left(uh\int_{\eta}^{\xi} Tv_s dz\right) + \frac{2C}{1+nC}uh\int_{\eta}^{\xi} T_1 v_s dz\right] \qquad \text{(Eqn.1b)}$$

$$\frac{1}{1+nC}u\frac{\partial v}{\partial s} + v\frac{\partial v}{\partial n} - \frac{C}{1+nC}u^2 = -g\frac{\partial \xi}{\partial s} - \frac{\tau_n}{\rho h} \qquad \text{(Eqn.1c)}$$

where, u and v are the depth average velocity components in the longitudinal and transverse directions respectively, g is the gravitational acceleration, ξ and η are the water surface and bed elevation from datum respectively, ρ is the density of the water, h is the depth of flow at any point, C is the curvature of the channel centerline and the z axis is considered positive upward. The channel centerline can be estimated:

$$C(s) = \frac{d\theta}{ds} = \frac{1}{r} \quad \text{(Eqn.2)}$$

where, θ is the deflection angle between the downstream direction and r the local radius of curvature. The two integral terms in Eqn.1b are the dispersion terms generated due to the redistribution of the momentum along the streamwise direction for the secondary flow in the river bend. In Eqn.1b, T_1 is the dimensionless shape function denoting the vertical fluctuation of longitudinal velocity and v_s is the secondary flow velocity in transverse direction. The individual river bend in a large river can be approximated as a part of sine-generated curve similar to the approach followed in analyzing the meandering channels (Langbein and Leopold, 1966). The periodic shape of the bend can be defined by the channel centerline angle (θ) with respect to down-valley direction and wavelength of the loop (Chen and Duan, 2006):

$$\theta = \theta_0 \cos(ks) \quad \text{(Eqn.3)}$$

where, $k = 2\pi/\lambda$, λ is the wavelength of the bend, θ_0 is the value of θ at the deflection point of the main channel. By assuming the ratio of the flow depth to the radius of channel curvature is small and neglecting the second order terms in Eqns. 1a-1c, the first order analytical solution for the streamwise velocity, considering the effect of dispersion terms in a sine generated curved channel, can be given as:

$$u = U + UNbk\theta_0\left[-\alpha\cos(ks) + \beta\sin(ks)\right] \quad \text{(Eqn.4)}$$

where, U is the reach-average velocity, b is the half width of the channel. The value of N ranges from positive unity at the outer bank to the negative unity at the inner bank. The parameters α and β can be estimated as follows:

$$\alpha = \frac{kHC_f\left(A + A_s + F^2 + 1\right)}{H^2k^2 + 4C_f{}^2} \quad \text{(Eqn.5a)}$$

$$\beta = \frac{2C_f{}^2\left(A + A_s + F^2 - 1\right) - H^2k^2}{H^2k^2 + 4C_f{}^2} \quad \text{(Eqn.5b)}$$

where, C_f is the Chezy's friction constant; F is the Froude number equal to $U/\sqrt{gH}$, H is the reach average flow depth, A is the scour factor characterizes the transverse bed slope, and A_s the momentum redistribution factor due to secondary current. However, the parameter A_s can be neglected for a mildly sinuous channel bends (δ <1.2), when the secondary flow is weak (Chen and Duan, 2006). Moreover, the analysis of the satellite imagery of Brahmaputra River indicates that the sinuosity of the braided loop ranges between 1 and 1.2 (Karmaker and Dutta, 2010b). Hence, the approximation for the mildly sinuous channel is valid for this study (Karmaker *et al*., 2010).

3.2 Fluvial Erosion Model

The fluvial erosion rate can be quantified using the excess shear stress theory proposed by Arulanandan et al. (1980):

$$\varepsilon = k_d\left(\tau_b - \tau_c\right)^a \quad \text{(Eqn.6)}$$

where ε is the fluvial erosion rate per unit time, k_d is the erodibility coefficient of the bank soil, τ_b is the boundary shear stress for the cohesive soil, τ_c is the critical shear stress and a the empirical exponent generally considered as unity. Erodibility parameters of the banks are highly variable and difficult to measure accurately (Rinaldi *et al*., 2008). In situ submerged jet testing device was used to estimate the erodibility parameters for the cohesive soils (Hanson and Simon, 2001; Karmaker and Dutta, 2011). The bed shear stress, as required by Eqn.6 can be estimated by using, $\tau = \gamma RS$, where, γ the unit weight of water, R the hydraulic radius, S the energy slope. Bank shear stress was estimated by using, $\tau_b = 0.76\gamma RS$, as suggested by Leutheusser (1963).

3.3 Stability and Cantilever Failure

Cantilever stability of the bank soil can be assessed by the combined effect of self-weight, shear strength, tensile strength and the compressive strength of the bank materials. The cantilever failure can occur in any of the three modes: (1) shear failure, (2) beam failure and (3) tensile failure. The factors of safety against these failures were computed using the formula as given by Thorne and Tovey (1981).

3.4 In Situ Bank Erosion Estimation

The river bankline migration rates of the bend at Jamuguri for four consecutive years from 2005 to 2008 were measured for the verification of model performance. The satellite imagery supplemented with DGPS (Differential Global Positioning System) survey data was used to estimate the annual bank erosion rate during the study period. Considering the observed probabilistic distribution of the bank soil erodibility and the return periods of the flood waves, the developed model has been simulated to estimate the stochastic bank erosion rates. These predicted bank erosions are finally verified with the observed bank erosion rate distribution of 45 major bends in the Brahmaputra River. The bank erosion rate was estimated by analyzing multi-date satellite imagery at annual scale. The images were collected from the open source image database supported by Global Land use and Cover Facility (GLCF). The yearly satellite imagery were stacked in chronological

order from 2005 to 2008 and the major channel bends were identified. The river bank lines were digitized manually using available tools in the image processing software. Then the average annual bank erosion rates were estimated from these annual bank line migration rates. The annual average bank erosion data are divided into a number of classes from zero to 150 m with 10 m increment. The cumulative distribution function of these annual bank erosion data was estimated and compared with the distribution of the bank erosion rate obtained from the model prediction.

4. Results and Discussion

4.1 Bank Soil Erodibility

The submerged jet tests conducted along the Brahmaputra River banks demonstrate that the critical shear stress and the erodibility coefficient are related (Karmaker and Dutta, 2011):

$$k_d = 3.16\tau_c^{-0.185} \quad \text{(Eqn.7)}$$

where, k_d is the erodibility coefficient in cm3(N-s)-1 and the critical shear stress in Pa.

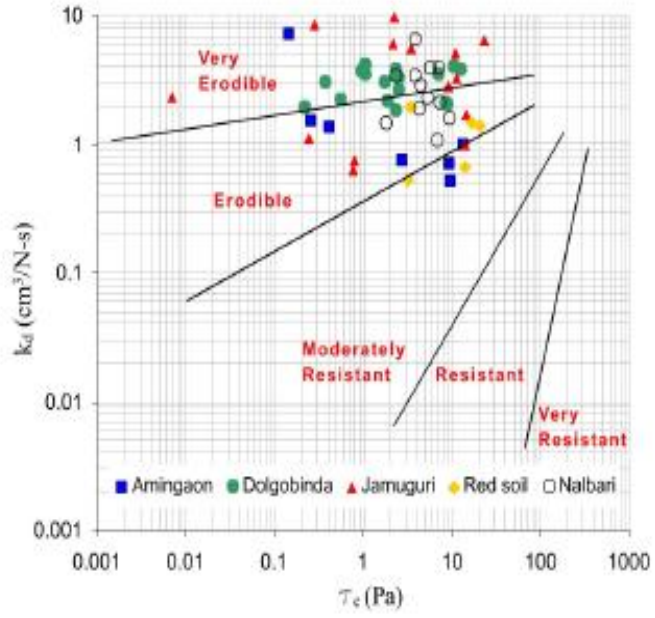

Fig 2. Soil erodibility determination through submerged jet test (Taken from Karmaker and Dutta, 2011)

The critical shear stress (τ_c) determined through the submerged jet test apparatus along the river Brahmaputra has the range 0.1-15 Pa. In order to find out its best random distribution, in-situ critical shear stress data were fitted with various probability distribution functions. The best distribution of the critical shear stress was found to follow the Gaussian probability function. The 58 sample points were grouped from 0-15 Pa with increment of 1 Pa. The co-relation coefficient is found to be 0.99 for this distribution (p = 0.007). The relationship between the critical shear stress and the erodibility coefficient developed is used here for estimation of k_d. The stochastic bank erosion estimation has been carried out considering the various probabilities of exceedence of critical shear stress and return period of the flood waves. The *in situ* critical shear stress of the fine soils can be determined through the submerged jet tests (Hanson and Simon, 2001; Hanson and Cook, 2004; Wynn, 2004; Karmaker and Dutta, 2011).

4.2 Seepage Erosion Model

Laboratory experiments were carried out for estimating seepage erosion with the soils from the composite river bank with similar stratification as found in-situ. Various combinations of bank stratifications with cohesive and cohesionless soils were investigated for different seepage gradients and the relationship between time and seepage gradient was determined for different bank stratifications (Karmaker and Dutta, 2013).

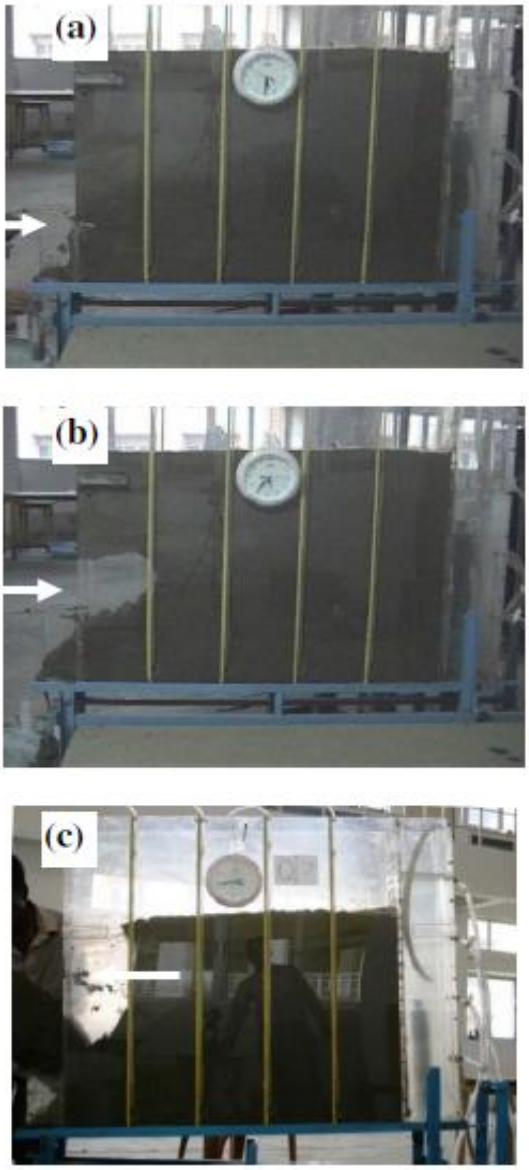

Fig 3. Seepage experiments (taken from Karmaker and Dutta, 2013)

A mathematical model for seepage erosion was formulated based on the results from the lysimeter experiments for composite riverbanks by considering subsurface flow similar in a confined aquifer. At time t = 0, both the stages at the river and groundwater were h0. The origin of the horizontal axis is at the intersection of the bank and the river, while the positive direction towards the bank. The storage in the silt layer is assumed negligible (Hantush and Jacob, 1955). Thus the governing equation for one-dimensional ground water flow in a composite bank can be given in Jiao and Tang (1999) provided the approximate solution to the one-dimensional ground water flow in a confined aquifer problem and within the domain between 0 and L, with boundary conditions,

$$h(x,0) = h_0 \qquad \text{(Eqn.8a)}$$

$$\text{and} \quad \lim_{x\to\infty} h(x,t) = h_0 \qquad \text{(Eqn.8b)}$$

where, S is the storativity, T is the transmissivity, h_f is the amplitude of the ith flood wave, ω the speed of flood wave. The seasonal stage hydrograph study was carried out by Karmaker and Dutta (2010) showed that monsoonal (seasonal) response (hs), is dependent on the basin average monsoonal rainfall (Rs) and. Based on the flood wave return period, h_f can be estimated from the historic stage record analysis (Karmaker and Dutta, 2010a). After fitting the individual flood wave and the monsoonal response with Maxwell distribution (1960), the synthetic stage hydrograph can be generated (Karmaker and Dutta, 2013). In order to apply the solutions provided by Jiao and Tang (1999) it is necessary to transfer the flood waves into the summation of sine functions. Thus the final form of flood hydrograph can be resolved as (Karmaker and Dutta, 2013):

$$h_r(t) = h_b + f_1(R_s)\left[\frac{t}{k_s}\exp\left(1-\frac{t}{k_s}\right)\right]^{r_s} + \sum_{i=1}^{n}\sum_{k=1}^{m} A_k \sin(\omega_k t_k + c_k) \qquad \text{(Eqn.9)}$$

where, $h_r(t)$ is the river stage at time t, hb the river stage before monsoon, ks and rs are the fitting parameters for monsoonal response, A_k, ω_k, c_k and t_k are the amplitude, frequency, phase shift and time period of the k th sinusoidal component of i th flood wave, respectively. The difference between the river stage [$h_r(t)$] and the ground water level h(x,t) produces the seepage head. To implement the equation (9) in equation (8a), h_0 is substituted with:

$$h_0 = h_b + f_1(R_s)\left[\frac{t}{k_s}\exp\left(1-\frac{t}{k_s}\right)\right]^{r_s} \qquad \text{(Eqn.10)}$$

The positive difference between groundwater level [h(x,t)] and the river stage [$h_r(t)$] at any time t gives the seepage head available. This head over the length (L) of the bank soil develops the seepage gradient (i_g). At the point, when the available seepage gradient is higher than the critical seepage gradient (ic), seepage flow occurs with the erosion of soil particles. This can be given as follows:

$$i_g = \left(\frac{h(L,t) - h_r(t)}{L}\right) \quad \text{for,} \quad h(L,t) > h_r(t) \qquad \text{(Eqn.11)}$$

Time required to bank collapse (tb) is a function of the seepage gradient and can be given as:

$$t_b = C(i_g)^{-k} \qquad \text{for,} \quad i_g > i_c \qquad \text{(Eqn.12)}$$

The above equation was found from the lysimeter experiments with physical model in laboratory. Daily seepage bank erosion (ε_t) can be estimated as:

$$\varepsilon_t = \frac{24\times 60}{f(i)} \times w_c \qquad \text{(Eqn.13)}$$

where, w_c is the average width of bank collapsed. The above equation has been developed considering the time to collapse (tb) in minutes. When the river stage is higher than the ground water, the water will seep towards bank; otherwise seepage flow will occur from the river bank. Numerical scheme consists of central difference over space for all other than first and last node along the streamline. The space along streamline was discritized at 50 m interval with a time interval of 1 hr, which is similar to the stage hydrograph recorded interval.

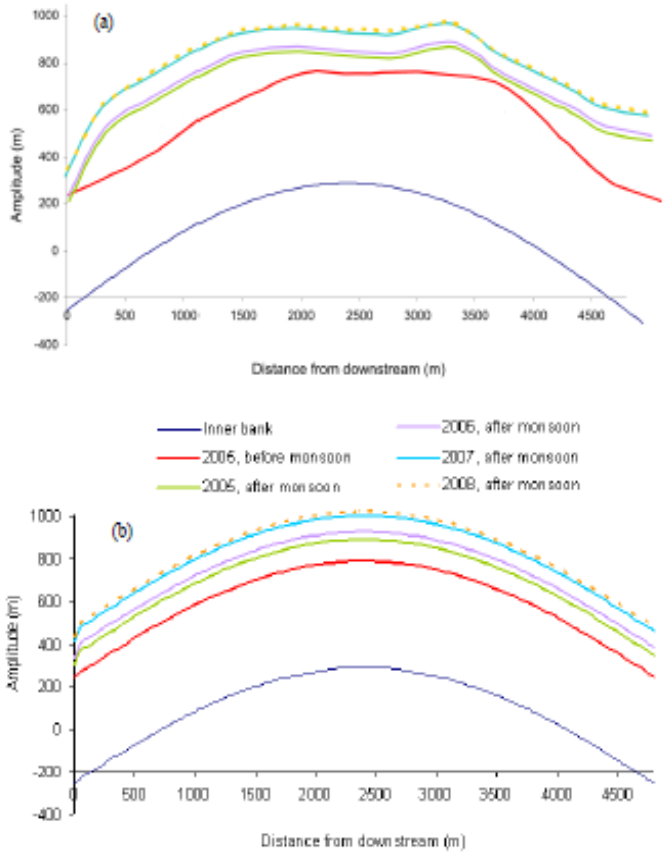

Figure 4. Predicted and observed bank erosion

4.3 Stochastic Erosion Prediction

The model was first validated at a river reach where the stage hydrograph, soil stratifications and the soil erodibility parameters were known (Karmaker, 2011) (Fig. 5). The validated model was then tested for the stochastic prediction of the bank erosion in cases, where the above parameters are unknown. The influence of the various parameters on the results of the model has been investigated. The parameters considered include: the monsoonal condition (dry, normal or wet), deflection angle (θ_0), longitudinal slope of river channel (S) and bed material size (d50).

4.4 Effect of Basin-Average Monsoon Rainfall

The predicted bank erosion rates during the dry monsoon season, indicate that the seasonal bank erosion rate is highly influenced by the return periods of flood waves. However, for the higher critical shear stress (probability of critical shear stress lower than 40%), the maximum annual bank erosion is dominated by seepage erosion. The seepage erosion rate found from the model simulations ranges between 1 and 6 m mainly depending on the return period of the flood waves. However, the annual bank erosion rate in the composite banks with fine soils of low critical shear stress and high erodibility coefficient are significantly affected by the return period of flood waves. The higher flood wave return period, more bank erosion rate.

The influence of normal monsoonal season with various return periods of flood waves was estimated. Interestingly, the basic nature of the maximum annual erosion rate is similar to the dry monsoon year. However, the predicted bank erosion rate is higher than that of dry monsoon condition. Although, the maximum annual bank erosion rate does not vary significantly with different return period of flood waves. The equilibrium state of the bank erosion indicates that even with very low critical shear stress in the bank fine soils, the seasonal maximum bank erosion will be within this range. In case of wet monsoon year, there is less influence of the different return period of flood waves. The limit of maximum annual bank erosion is higher than that of normal and dry condition. The predicted maximum annual erosion rate is about 120 m with a 20-year return period of flood wave. Moreover, the annual erosion has not reached to any equilibrium limit. This indicates with lower critical shear stress of the bank fine soils higher bank erosion rate is expected for wet monsoon years. The predicted maximum annual bank erosion increased to 80% from dry to wet monsoon season.

Moreover, the simulated results for different flood wave return periods showed that near bank bed level was almost same for different return period of flood waves. This essentially indicates that the equilibrium bed scour solely depends on the bank soil and bed material characteristics.

4.5 Evaluation of Stochastic Bank Erosion Prediction

The cumulative distribution of the bank erosion simulated by the model was used to evaluate the model performance in its stochastic prediction. Therefore, all the simulation results mentioned in the previous sections were considered as the sample dataset. The observed annual bank erosion rates obtained from satellite imagery analysis were considered for the evaluation.

For analysis of the observed annual bank erosion, the river reach was divided into two regions: (i) from the confluence of the Lohit, Siang and Dibang to Guwahati, and (ii) downstream of Guwahati to Indo-Bangladesh border. The average annual bank erosion rate in the period 2005-2008 was ~87 m at the upstream of Guwahati, whereas, the average annual bank erosion was found to be ~68 m at its downstream. The analysis also shows that the most of the wavelengths of the braided loop lie in between 9000 and 12000 m with an average of ~10,000 m. The envelope of the predicted bank erosion is shown in Fig. 5 with dash lines. The cumulative probability distribution of the observed bank erosion was computed and plotted in the same figure. Interestingly, the stochastic erosion predict follows fairly the observed distribution, close to the upper bound of the envelope.

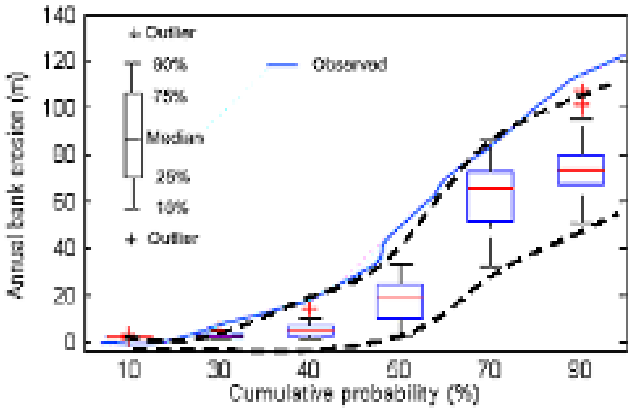

Figure 5: Observed and simulated distribution of the bank erosion (Taken from Karmaker and Dutta, 2014)

However, the satellite imagery analysis indicates the annual bank erosion rate, which also includes the erosion during the non-monsoon periods. During the non-monsoon periods, the bank erosion is mainly due to sub-aerial erosion and bank collapse due to poor cohesion. In addition, the average bank height was considered for the prediction of the stochastic bank erosion. Interestingly, the orders of the observed and predicted bank erosion match fairly well. Thus, the stochastic bank erosion prediction from the present model can be used to identify the vulnerable river reaches under the threatening of the bank erosion.

CONCLUSIONS

The present study has analyzed the annual erosion rate of composite river banks with its controlling parameters and their probability distribution. This model uses an analytical hydrodynamic and sediment transport model with the

dominated bank erosion processes in a composite river bank. The main bank erosion processes in the composite river bank include basal erosion, seepage erosion through coarse soil layers, and mass collapse mechanisms. The spatial variation of the critical shear stress of the fine soil layers of the river bank plays an important role for the spatial variation in the annual bank erosion rate. Fluvial erosion with subsequent bank collapse mechanism was found as major bank erosion processes in the composite river bank. However, seepage erosion was dominant when the critical shear stress of the bank soil is of high magnitude. However, one major limitation of the model is that it considers the similar stratification of the bank soil and the each soil layers has similar hydraulic and soil properties. However, in future, it is required to investigate the effects of the soil density and hydraulic parameters on the bank erosion.

REFERENCES

[1]. Arulanandan, K., Gillogley, E., and Tully, R. (1980). "Development of a quantitative method to predict critical shear stress and rate of erosion of natural undisturbed cohesive soils." Tech. Report GL-80-3. Vicksburg, Miss., U.S. Army Corps of Engineers.

[2]. Blondeaux, P. and Seminara, G. (1985). "A unified bar-bend theory of river meander." J. Fluid Mech., Cambridge, U. K., 157, 449-470.

[3]. Chen, D. and Duan, J. G. (2006). "Modeling width adjustment in meandering channels." J. Hydrologic. Engg., 321, 59-76.

[4]. Chien, N., Zhang, R. and Chou, Z. D. (1989). "River evolution." Chinese Scientific Press, Beijing, China (in Chinese).

[5]. Darby, S. E., Rinaldi, M. and Dapporto, S. (2007). "Coupled simulation of fluvial erosion and mass wasting for cohesive river banks." J. Geophys. Res., 112, F03022; DOI: 10.2029/2006JF000722.

[6]. Darby, S. E. and Thorne, C. R. (1996). "Numerical simulation of widening and bed deformation of straight sand-bed rivers. I: Model development." J. Hydra. Engg., ASCE, 122(4), 184-193.

[7]. Darby, S. E., Thorne, C. R. and Simon, A. (1996). "Numerical simulation of widening and bed deformation of sand-bed rivers. II: Model evaluation." J. Hydrologic. Engg., ASCE, 122(4), 194-202.

[8]. Duan, J. G. (2005). "Analytical approach to calculate rate of bank erosion." J. Hydrologic. Engg., 131(11), 980-990.

[9]. Duan, G., Jia, Y. and Wang, S. (1997). "Meander process simulation with a two dimensional numerical model." Proc., Conf. on Mgmt. of Landscapes Distributed by Channel Incision, University of Mississippi, Miss., 389-394.

[10]. Engelund, F. (1974). "Flow and bed topography in channel bends." J. Hydr. Div., ASCE, 100(HY11), 1631-1648.

[11]. Fox, G.A., and Wilson, G.V. (2010). "The role of subsurface flow in hillslope and stream bank erosion: A review." Soil Sci. Society of America Journal, 74(3), 717-733.

[12]. Fox, G.A., Wilson, G.V., Periketi, R.K., and Cullum, B.F. (2006). "A sediment transport model for seepage erosion of streambanks." J. Hydrologic Engg., 11(6), 603–611.

[13]. Fox, G. A., Wilson, G. V., Simon, A., Langendoen, E., Akay, O and Fuchs, J. W. (2007). "Measuring streambank erosion due to ground water seepage: correlation to bank pore water pressure, precipitation and stream stage." Earth Surf. Processes Landforms, 32, 1558-1573; DOI:10.1002/esp.1490.

[14]. Hanson, G. J. and Cook, K. R. (2004). "Apparatus, test procedures, and analytical methods to measure soil erodibility in situ." Applied Eng. in Agric., 20(4), 455-462.

[15]. Hanson, G. J. and Simon, A. (2001). "Erodibility of cohesive streambeds in the loess area of the Midwestern USA." Hydrological Processes, 15(1), 23-38.

[16]. Hantush, M.S. and Jacob, C.E. (1955). "Non-steady radial flow in an infinite leaky aquifer." Eos Trans., AGU 36(1), 95-100.

[17]. Ikeda, S., Parker, G and Sawai, K. (1981). "Bend theory of river meanders. Part 1." Linear development. J. Fluid Mech., Cambridge, U.K., 112, 363-377.

[18]. Ikeda, S. (1989). "Sediment transport and sorting at bends. In: Flow in Meandering Channels." (Eds.) Ikeda, S., Parker, G. American Geophysical Union, 103-125.

[19]. Johannesson, H. and Parker, G. (1989). "Velocity redistribution in meandering rivers." J. Hydraulic Engg., 115(8), 1019-1039.

[20]. Jiao, J.J. and Tang, Z. (1999). "An analytical solution of groundwater response to tidal fluctuation in a leaky confined aquifer." Water Resour. Res. 35(3), 747-751.

[21]. Karmaker, T. and Dutta, S. (2009). "Predicting vulnerable bank erosion zones in a large river meander." Proc. of Water, Environment, Energy and Society (WEES)-2009, New Delhi. 1670-1676.

[22]. Karmaker, T. and Dutta S. (2010a). "Generation of synthetic flood hydrograph in a large river basin." J. Hydrology, 381(3-4), 287-296.

[23]. Karmaker, T. and Dutta, S. (2010b). "Composite bank erosion modeling in an alluvial river bend." Proc. of River Flow 2010, IAHR International conference, 8-10 Sept, Germany, 1315-1322.

[24]. Karmaker, T. and Dutta S. (2011). "Erodibility of fine soil from the composite river bank of Brahmaputra in India." Hydrological Processes, 25, 104-111.

[25]. Karmaker, T. and Dutta, S. (2013). "Modelling seepage erosion and bank retreat in the composite riverbank." J. Hydrology, 476, 178-187.

[26]. Karmaker, T., & Dutta, S. (2014). Stochastic erosion of composite banks in alluvial river bends. Hydrological Processes, 1339(July 2014), 1324–1339. doi:10.1002/hyp.10266.

[27]. Karmaker, T., Ramaprasad, Y. and Dutta, S. (2010). "Sediment transport in an active erodible bend of

Brahmaputra River." Shadhana, Academy Proceedings, 35(6), 693-706.

[28]. Kikkawa, H., Iheda, S. and Kitagawa, A. (1976). "Flow and bed topography in curved open channels." J. Hydraul. Divv., ASCE, 109(9), 1327-1342.

[29]. Kovacs, A. and Parker, G. (1994). "A new vectorial bedload formulation and its application to the time evolution of straight river channels." J. Fluid Mech., Cambridge, U. K., 267, 153-183.

[30]. Langbein, W. B. and Leopold, L. B. (1966). "River meanders: Theory of minimum variance." U.S. Geological Survey Professional Paper No. 422-H, pp-18.

[31]. Langendoen, E. J. (2000). "CONCEPTS-Conservational channel evolution and pollutant transport system." Research Report No. 16, US Department of Agriculture, Agricultural Research Service, National Sedimentation Laboratory, Oxford, MS.

[32]. Lawler, D. M. (1995). "The impact of scale on the processes of channel-side sediment supply: A conceptual model. In: Effects of scale on Interpretation and Management of Sediment and Water Quality (Proc. of a Boulder Symp.)." IAHS Publ. 226, Wallingford, U.K.: International Assoc. of Hydrological Science, 175-184.

[33]. Lawler, D. M., Thorne, C. R. and Hooke, J. M. (1997). "Bank erosion and stability. In: Applied Fluvial Geomorphology for River Engineering and Management" Thorne, C.R. et al., (eds.) 137-172. J. Wiley, Chichester, U. K.

[34]. Leutheusser, H. J. (1963). "Turbulent flow in rectangular ducts." J. Hydraul. Div., ASCE, 89, 1-19.

[35]. Maxwell, J.C. (1960). "Quantitative geomorphology of the San Dimas Experimental forest, California." Project ONR 389-042, Tech. report-19, Dept. of Geology, Columbia Univ., New York.

[36]. Midgley, T. L., Fox, G. A. and Heeren, D. M. (2012a). "Evaluation of the bank stability and toe erosion model (BSTEM) for predicting lateral retreat on composite streambanks." Geomorphology, 145-146, 107-114.

[37]. Midgley, T. L., Fox, G. A., Wilson, G. V., Heeren, D. M., Langendoen, E. J. and Simon, A. (2012b). "Seepage-induced streambank erosion and instability: In-situ constant head experiments." J. Hydrol. Engg. doi.10.1061/ (ASCE) HE 1943-6584.0000685.

[38]. Mosselman, E., Huisink, M., Koomen, E. and Seijmonsbergen, A.C. (1995). "Morphological changes in a large braided sand-bed river." River Geomorphology, E. J. Hickin, (ed.), Wiely, Chiehester, U.K., 235-247.

[39]. Muramoto, Y. and Fujita, Y. (1992). "Recent channel processes of the major rivers in Bangladesh." Annuals of the Disaster Prevention Res. Inst., Kyoto, Japan, 35 B-2, 89-114 (in Japanese)

[40]. Nagata, N., Hosoda, T. and Muramoto, Y. (2000). "Numerical analysis of river channel processes with bank erosion." J. Hydro. Engg., ASCE, 126(4), 243-252.

[41]. Nardi, L., Rinaldi, M. and Solari, L. (2012). "An experimental investigation on mass failures occurring in a riverbank composed of sandy gravel." Geomorphology, 163-164, 56-69.

[42]. Parker, G., Sawai, K. and Ikeda, S. (1982). "Bend theory of river meanders. Part 2. Nonlinear deformation of finite-amplitude bends." J. Fluid Mech., Cambridge, U.K., 115, 303-314.

[43]. Rinaldi, M., Casagli, S., Dapporto and Gargini, A. (2004). "Monitoring and modelling of the pore water pressure changes and riverbank stability during flow events." Earth Surf. Processes landforms, 29, 237-254.

[44]. Rinaldi, M., Mengoni, B., Luppi, L. and Darby, S. E. (2008). "Numerical simulation of hydrodynamics and bank erosion in a river bend." Water Resour. Res., 44, W09428; DOI: 10.1029/2008WR007008.

[45]. Rinaldi, M., and Nardi. (2012). "Modeling interactions between river hydrology and mass failures." J. Hydrol. Engg. (In press)

[46]. Simon, A., Curini, A., Darby, S. E. and Langendoen, E. J. (2000). "Bank and near-bank processes in an incised channel." Geomorphology, 35, 183-217.

[47]. Thorne, C. R., Russel, A. P. G. and Alam, M.K. (1993). "Planform pattern and channel evolution of Brahmaputra River, Bangladesh, In: Braided Rivers." J.L. Best, and C.S. Bristow (Eds.) Geological Society of London (Spl. Publication), London, 157-276.

[48]. Thorne, C. R., and Tovey, N. K. (1981). "Stability of composite river banks." Earth Surf. Proc. and Landforms, 6, 469-484.

[49]. Tingsanchali, T. and Chinnarasri, C. (1997). "Design of Mekong river bank protection." Proc. Conf. on Mgmt. of Landscapes Distributed by Channel Incision, University of Mississippi, Miss., 345-348.

[50]. Wilson, G.V., Periketi, R.K., Fox, G.A., Cullum, R.F. and Shields, F.D. (2007). "Seepage erosion properties contributing to streambank failure." Earth Surf. Processes Landforms, 32, DOI: 10.1002/esp.1405.

[51]. Wynn, T. (2004). "The effects of vegetation on streambank erosion." PhD thesis, Blacksburg, Va, Virginia Tech, Department of Biological Systems Engineering.